# Catalytic allylation of phenols : chloride-free route towards epoxy resins

Rijn, J.A. van

# 7

# Theoretical study on the mechanism of $[RuCp(PP)]^+$-catalyzed allylation of phenol with allyl alcohol

**Abstract**
The two steps in the mechanism of catalytic allylation reaction determining activity and selectivity are an oxidative addition and reductive elimination, respectively. The intermediates, proposed in the previous chapters to play a key role in these steps, have been modelled using Density Functional Theory. The relative energies of the intermediates as a function of the phosphine ligand present on the ruthenium centre are discussed and the results nicely illustrate the role of the ligand in the stabilization of certain intermediates. Calculations were made for the situation in the absence as well as in the presence of acid. Several observations made from experiments in previous chapters are reflected in the energy calculations. In some instances entropic effects must also play a significant role. However, the DFT computational method used does not take entropy into consideration.

## 7.1 Introduction

In the previous chapters, the performance of cationic $[Ru(II)Cp(PP)]^+$ complexes as catalysts for the O- and C-allylation of phenols with allyl alcohol is discussed. Both the activity and selectivity in the catalytic allylation of phenols strongly depend on the structural characteristics of the complexes, and in particular on those of the bidentate phosphine ligands. It appeared that initially formed O-allylated products can be consecutively converted into C-allylated phenolic products, but the rate of this reaction also strongly depends on the structure of the catalyst. Addition of catalytic quantities of strong acid to the catalyst system not only leads to increased activity in the allylation reaction, but also affects the selectivity of the reaction.

Most of the publications on ruthenium-catalyzed allylation do not address the precise mechanism of either O- or C-allylation.[1-4] Often the role of the ligands is overlooked, whereas it was shown in the previous chapters to be crucial for both activity and selectivity.

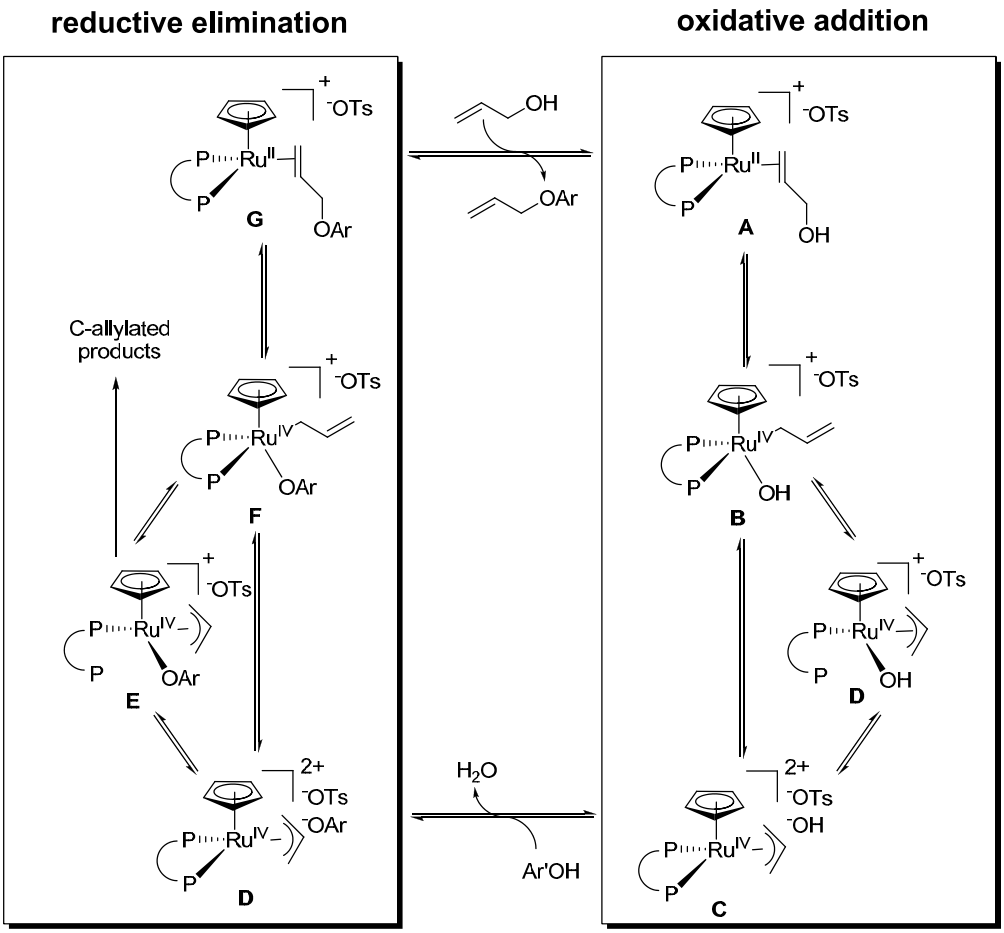


**Scheme 7.1.** Proposed catalytic cycle for allylation of phenols with allyl alcohol in the presence of $[RuCp(PP)]^+$ catalysts.

Furthermore σ- to π-allyl isomerization, a known process for these reactions,[5] is often not discussed and only the supposedly more stable π-allyl species are described. It has been suggested that for both O- as well as C-allylation the nucleophile attacks the coordinated π-allyl group from outside the coordination sphere.[2,4] However, with the Ru-diphosphine complexes described in this thesis, it is impossible to consistently relate outside nucleophilic attack on the π-allyl moiety of these complexes with the experimentally observed effects of, in many cases subtle, structural variations of the diphosphine ligands on these complexes' catalytic activity and selectivity in phenol allylation.

In this chapter, a more detailed study is described on the proposed mechanism of the ruthenium catalyzed O- and C-allylation of phenol (Scheme 7.1) as a function of the ligand structure of the catalyst. Possible intermediates are discussed and compared by means of DFT calculations, in particular those involved in the oxidative addition, which are related to the activity, and those of the reductive elimination, which determine the selectivity to the final product. Although several papers have reported calculations on allylation reactions,[6-8] none of these address the strong effects of the bidentate phosphine ligand on the rate and selectivity of these reactions.

## 7.2 Results and discussion

### *7.2.1 Overall reaction energies*

In order to obtain a better insight in the thermodynamics of the two major reactions taking place in the catalytic allylation of phenol (Scheme 7.2), the overall reaction energies were first determined using DFT molecular calculations.

The formation of phenyl allyl ether (Scheme 7.2a) has an ΔE of +0.1 kcal/mol, while the formation of *ortho*-allylphenol has an ΔE of –8.8 kcal/mol (Scheme 7.2b). The C-allylated product therefore is the thermodynamic end-product of allylation, while the O-allylated product is a kinetic product.

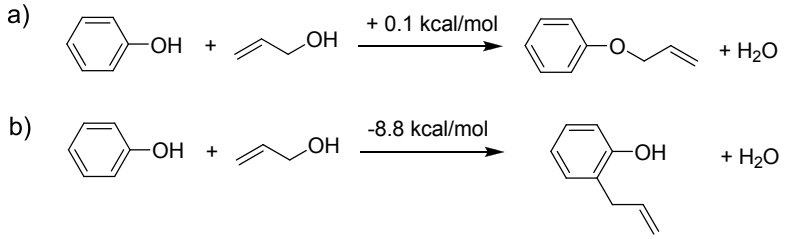


**Scheme 7.2.** Calculated reaction energies for O- and C-allylation of phenol with allyl alcohol.

It is indeed experimentally observed that at longer reaction times, O-allylated product is ultimately converted into the thermodynamic C-allylated end-product (Chapter 2). The rate of this conversion however, strongly depends on catalyst structure and experimental conditions. The calculated almost thermo-neutrality of O-allylation is in agreement with the observed partial conversion of substrates to O-allylated product and the reversibility of O-allylation. A higher than thermodynamic conversion to O-allylated product can only be achieved if the reaction product water is removed from the reaction medium, e.g. by phase separation (Chapters 2 and 3).

### *7.2.2 Oxidative addition of allyl alcohol*

For the oxidative addition of allyl alcohol to Cp-ruthenium complexes with bidentate phosphine ligands (**1**) (Scheme 7.3), it is proposed that a σ-allyl species is initially formed (**2**), followed by a σ/π-allyl isomerization. Itoh and co-workers have reported a study on the oxidative addition of allyl halides to Cp-ruthenium complexes with two mono-phosphine ligands.[5] By means of NMR spectroscopy it was found that upon oxidative addition a σ-allyl species is initially formed which can proceed to a π-allyl species after dissociation of one of the phosphine ligands. For the Ru-based system described in this thesis, in order to prevent an undesired 20-electron species when the π-allyl species is formed, indeed one of the phosphines may dissociate, forming species **3**. Otherwise the hydroxide anion can be expelled from the coordination sphere to maintain an 18-electron species (**4**). Finally, ring slippage of the Cp anion from $\eta^5$- to $\eta^3$-coordination[9] would also give an 18-electron species with a

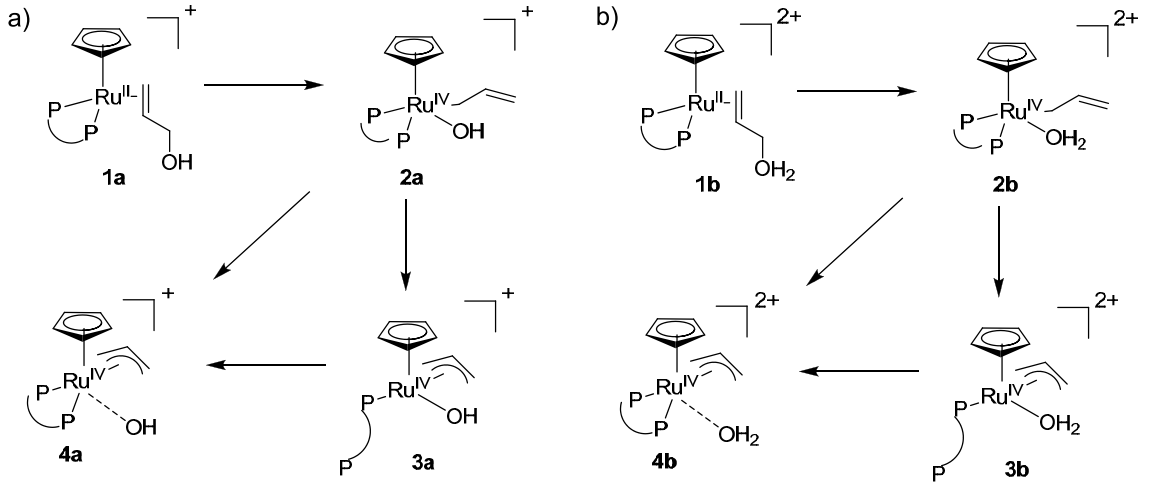


**Scheme 7.3**. Proposed intermediates in the oxidative addition of allyl alcohol for a) monocationic complexes in the absence of acid or b) dicationic complexes in the presence of acid. Solid bonds indicate coordination bonds, while dashed bonds represents bonds longer than coordination bonds.

π-allyl and a coordinating hydroxyl group. However, this species is very high in energy (energy difference relative to **1** ≥ 49 kcal/mol), as was determined by means of DFT-calculations, which seems to be an unlikely event and was not taken into further consideration.

Basset and co-workers have described the oxidative addition of allyl alcohol to a palladium(0) catalyst, both in neutral and acidic conditions. It was found that in the absence of strong acid, hydroxyl anions are produced, while in an acidic medium these hydroxyl anions rapidly react with the excess of protons to form water.

For the present ruthenium(II) catalyst system it is proposed that in a non-acidic system oxidative addition of allyl alcohol occurs without protonation of the Ru-bound allyl alcohol *a priori*. Addition of a strong acid, like *p*-toluenesulfonic acid (HOTs), accelerates the reaction in a major way. A strong acid will protonate the allyl alcohol during oxidative addition, thus facilitating this step by transforming the poor hydroxyl leaving group into the good leaving group water. Therefore, two different types of complexes have been calculated: one in the absence of acid (Scheme 7.3a) and one in the presence of acid (Scheme 7.3b). In order to save calculation time, the phenyl groups on phosphorous were replaced by hydrogens. This means that steric and electronic effects of substituents at P are not taken into account. The structure of the backbone of diphosphine ligands at Ru was experimentally shown to have a decisive influence on the activity and selectivity in phenol allylation. As in the actual ligands used the same or similar substituents at P are being used, it is believed that computation of energy profiles of catalytic pathways of model cationic catalyst complexes, $[(Cp)(H_2P(CH_2)_nPH_2)Ru(II)]^+$ will provide useful comparative insights into the effects of the diphosphine backbone structure on the catalytic performance of real catalyst complexes. Since DFT does not easily allow calculation of energy differences due to actual protonation events, the energy schemes shown were calculated for a completely monocationic complex catalytic pathway (Scheme 7.3a), simulating acid-free conditions or a completely dicationic complex pathway (Scheme 7.3b), simulating acidic conditions. In practice only a catalytic quantity of acid is applied and the acid will only play a co-catalytic role in converting certain intermediates.

### *7.2.3 Structural properties*

The calculated molecular structures **2a**-**4a** and **2b**-**4b** are shown in Figure 7.1 for structures with a $C_2$-bridge in the phosphine bidentate ligand (1,2-diphosphinoethane = dpe). The

**Table 7.1**. Lengths of coordination bonds in calculated structures **2a**-**4b** for Ru(IV)Cp complexes with dpe as bidentate phosphine ligand.

| | Bond lengths (Å) | | | | | |
|---|---|---|---|---|---|---|
| Structure | Ru1-O2 | Ru1-P3 | Ru1-P4 | Ru1-C5 | Ru1-C6 | Ru1-C7 |
| **2a** | 2.156 | 2.316 | 2.314 | 2.240 | 3.075 | 4.020 |
| **3a** | 2.018 | 2.355 | 6.567 | 2.243 | 2.186 | 2.229 |
| **4a** | 2.954 | 2.612 | 2.296 | 2.388 | 2.202 | 2.233 |
| **2b** | 2.222 | 2.383 | 2.358 | 2.352 | 3.192 | 4.102 |
| **3b** | 2.264 | 2.462 | 6.540 | 2.271 | 2.219 | 2.292 |
| **4b** | 4.669 | 2.402 | 2.346 | 2.357 | 2.246 | 2.308 |

structures of the complexes with different chelating ligands dpm (= diphosphinomethane) and dpb (= 1,4-diphosphinobutane), show very similar geometrical characteristics and will not be discussed in detail. Selected calculated bond distances for the ruthenium complexes with the ligand dpe are listed in Table 7.1.

In the calculated Ru(IV) structures **2a**-**2b** σ-allyl coordination is present; only one carbon of the allyl group is within coordination distance from the Ru1 centre. In **3a**-**3b** one of the phosphine donor atoms is dissociated, and in **4a**-**4b** hydroxyl or water dissociation has occurred. For the structures **2** and **3**, the Ru1-O2 distance shows a typical coordination bond distance, but in structures **4a** and **4b**, the O2 atom is expelled from the Ru1 coordination sphere, to a distance of 2.9 and 4.7 Å, respectively. When the structures of **3a-3b** and **4a-4b** are compared with respect to the π-allyl group, it is observed that for the **3a-3b** structures an endo-allyl orientation is favored, while for **4a-4b** an exo-allyl orientation is found in the

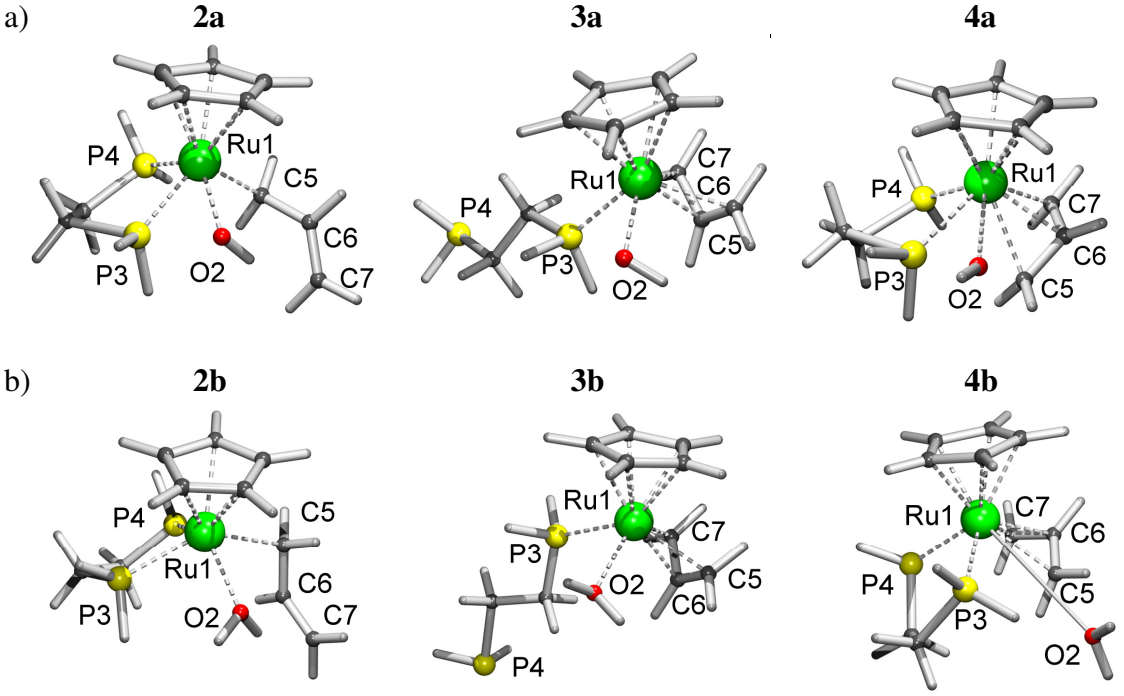


**Figure 7.1**. Calculated structure of **2**, **3** and **4** as a) monocationic species (absence of acid) and b) dicationic complexes (presence of acid).

minimized structure.

Another feature of the structure of **4a** is that the coordination of the two phosphine donors is not symmetric (Ru1-P3: 2.612 Å and Ru1-P4: 2.296 Å). The calculated local energy minimum apparently requires some mode of dissociation for one of the phosphine donors. This asymmetry is also influenced by the position of the hydroxyl anion. The O2-P3 distance is very short (1.762 Å) and apparently the anion interacts with the slightly electropositive phosphine donor. This interaction is observed for all the structures calculated, both with a hydroxyl anion as well as a phenolate anion. The calculation method does not allow complete dissociation of the anion from the cationic complex. Such features are not observed in the structure of **4b**, because the water molecule in this complex is clearly removed from the coordination sphere of the ruthenium centre (Ru1-O2 = 4.669 Å).

### *7.2.4 Energy diagrams for oxidative addition*

The energy diagrams for oxidative addition of complexes with the ligands dpm, dpe, and dpb are shown in Scheme 7.4, both for the monocationic complex (Scheme 7.4a; absence of acid) as well as for the dicationic complex (Scheme 7.4b; presence of acid).

**The cationic [RuCp(PP)(allyl alcohol)]$^+$ system**

For the complex [RuCp(dpm)]$^+$ in the absence of acid, it is clear that phosphine dissociation gives the most stable Ru(IV) complex (**3a**). The strained 4-membered ring favors to open after oxidative addition to provide coordination space for π-allyl coordination. The preferred dissociation of one of the phosphine donors in a strained 4-membered chelate ring of a dpm ligand was observed in calculations on a Pd(dpm)-catalyzed Heck-type reaction.[10] A direct reaction from species **1a** to **3a** seems unlikely.[5]

The energy difference of +34.8 kcal/mol for oxidative addition seems to correspond with the observation that reaction temperatures of about 100 °C are needed for a reasonable reaction rate. The σ-allyl species with structure **2a** can thus probably be regarded as being close to the activated transition state barrier for the conversion of **1a** to **3a** or **4a**.

Phosphine dissociation is very likely to occur (from **2a** to **3a** = –16.1 kcal/mol) on forming a π-allyl species. Alternatively, and with a similar likelihood, dissociation of the basic hydroxide anion takes place to generate species **4a** (**2a** to **4a** = –14.2 kcal/mol).

The behavior of [RuCp(dpe)]$^+$ is somewhat different from that of [RuCp(dpm)]$^+$ in the absence of acid, showing no clear preference for any of the species (**2a**, **3a** or **4a**) formed after

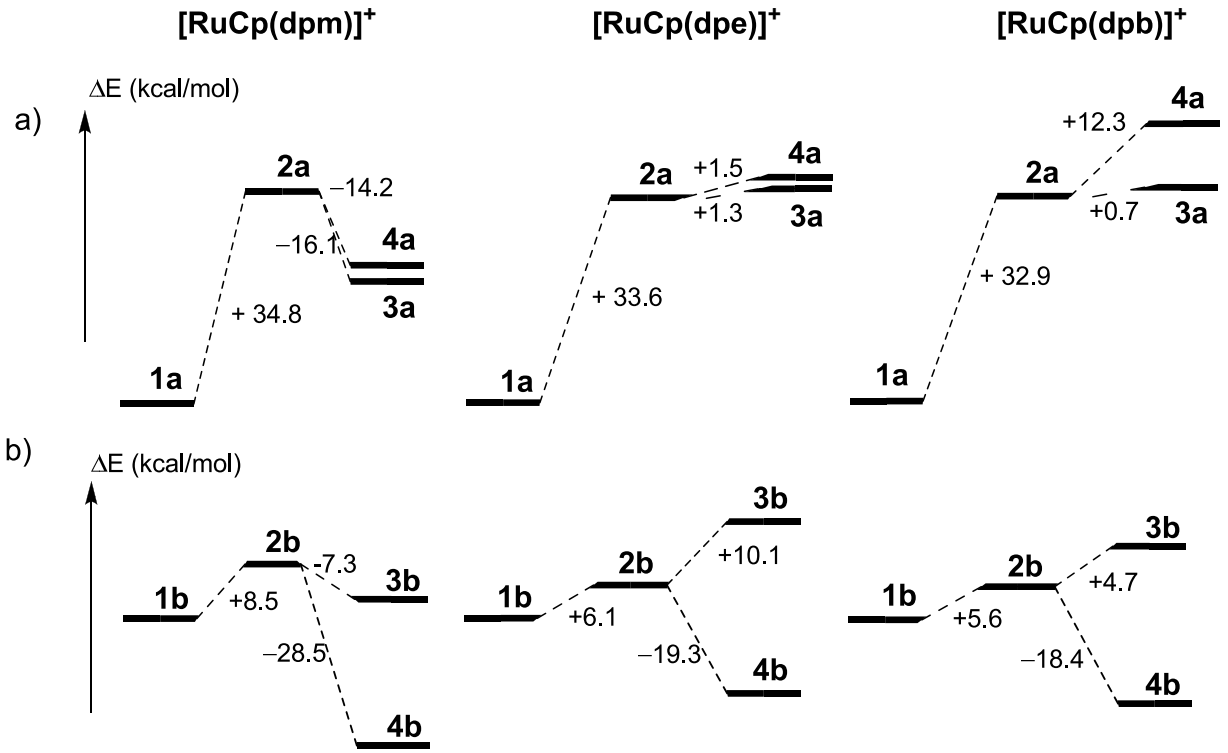


**Scheme 7.4**. Energy diagrams for the oxidative addition step for [RuCp(PP)(allyl alcohol)]$^+$ complexes **1** in the a) absence of acid and b) presence of acid.

oxidative addition; both π-allyl species **3a** and **4a** are comparatively destabilized relative to σ-allyl species **2a**. This can be seen as a consequence of the larger P-Ru-P bite angle of the $C_2$ backbone bidentate phosphine ligand relative to dpm, which leads to less space available for coordination of the π-allyl moiety (occupying two binding sites) at Ru, and thus to destabilization of these species. The energy differences for these species are very small and interconversion between them are very well possible.

Finally, for the complex [RuCp(dpb)]$^+$ a similar energy difference between **1a** and **2a** (+ 32.9 kcal/mol) is observed as for both [RuCp(dpm)]$^+$ and [RuCp(dpe)]$^+$. Again, due to an even larger P-Ru-P bite angle of the $C_4$-diphosphine, the π-allyl species **3a** and, in particular **4a,** are raised in energy. The higher energy of species **4a** reflects that the coordination space at Ru is barely sufficient to accommodate the distant coordination of the anion with the coordination of both two bidentately coordinating entities, i.e. the $C_4$ backbone diphoshine and the π-allyl moiety. The coordination of both phosphine moieties is forced into an unsymmetrical coordination with different Ru-P distances, while the hydroxide anion is at close distance from one of the P donors.

**The dicationic [RuCp(PP)(allyl alcohol + H)]$^{2+}$ system**

In the protonated dicationic species, simulating the presence of acid, the trends in the energy profiles of oxidative addition are significantly less dependent on the ligand (Scheme 7.3b, Figure 7.1b, Scheme 7.4b). This is in part a consequence of the DFT computational method in which only energy differences between fully protonated (or fully deprotonated) species can be calculated, while the protonation event itself cannot be considered.

The calculated energy difference between **1b** and **2b** is much smaller than between corresponding species **1a** and **2a** in the absence of added acid for all three of the complexes. The low energy barrier **1b** → **2b** demonstrates that formation of neutral $H_2O$ drives the protonation in **2b** and it can thus be rationalized that the complexes strongly prefer to expel the water molecule from the coordination sphere forming dicationic species **4b** (–28.5 kcal/mol for [RuCp(dpm]$^{2+}$ and about –19 kcal/mol for [RuCp(dpe)]$^{2+}$ and [RuCp(dpb)]$^{2+}$) compared to phosphine dissociation species (**3b**). For the [RuCp(dpm)]$^{2+}$ complex, stronger stabilization of intermediate **4b** due to the small P-Ru-P angle (thus providing more space for (bidentate) π-allyl formation), is clearly reflected.

**Allylation vs isomerization**

The [RuCp(dppb)]$^{+}$ complex was experimentally demonstrated to be only active for allylation in the presence of strong acid (Chapter 2), where oxidative addition is highly promoted (**1b** to **2b** = +5.6 kcal/mol). In the absence of acid, [RuCp(dppb)]$^{+}$ is an active catalyst in the isomerization of allyl alcohols into carbonyl compounds, where phosphine dissociation from a Ru(II) is proposed to be an elementary step in the catalytic cycle.[11] Not only does the presence of acid promote the oxidative addition, but at the same time the allyl alcoholate formation (Scheme 7.5) will be inhibited in the presence of a strong acid. It is the combination of these two effects of acid that makes this catalyst system potentially attractive for the O-allylation of phenols. In non-acidic environment the bidentate coordination of allyl alcoholate, inducing phosphine dissociation has a relative low energy difference (+5.8 kcal/mol; Scheme 7.5) compared to the products of oxidative addition in the absence of strong acid **2a**-**4a**.

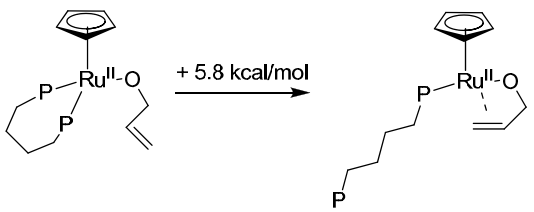


**Scheme 7.5.** Energy difference for phosphine dissociation during allyl alcohol isomerization into propanal.

However, when the reaction shown in Scheme 7.5 is calculated for complexes with the other ligands (dpm and dpe), also energy differences considerably lower than that of the oxidative addition step in the absence of acid are found (as low as −2.5 kcal/mol for dpm). Nevertheless, these complexes are experimentally found not to be active in the isomerization of allyl alcohol into propanal under the reaction conditions used for the allylation reactions (Chapter 2). The backbone flexibility of bidentate ligands with a relatively long (flexible) backbone is considered to be higher than that of ligands with a shorter backbone and thus phosphine dissociation will be relatively more likely. However, the backbone flexibility of the ligand will be reflected in an entropic factor of the free energy, which is not taken into consideration with the calculation method used. The degrees of freedom the reaction shown in Scheme 7.5, is probably greater for the complexes with a $C_4$-backbone ligand than that of complexes with shorter ligand backbones, thus favoring the isomerization reaction over the allylation reaction.

### *7.2.5 Reductive elimination towards O- and C-allylated products*

After exchange of the hydroxyl for a phenolate anion, similar isomers will be formed as discussed for the hydroxyl-containing species (Scheme 7.6). Due to the high electrostatic interaction between the positively charged ruthenium(IV) center and the negatively charged

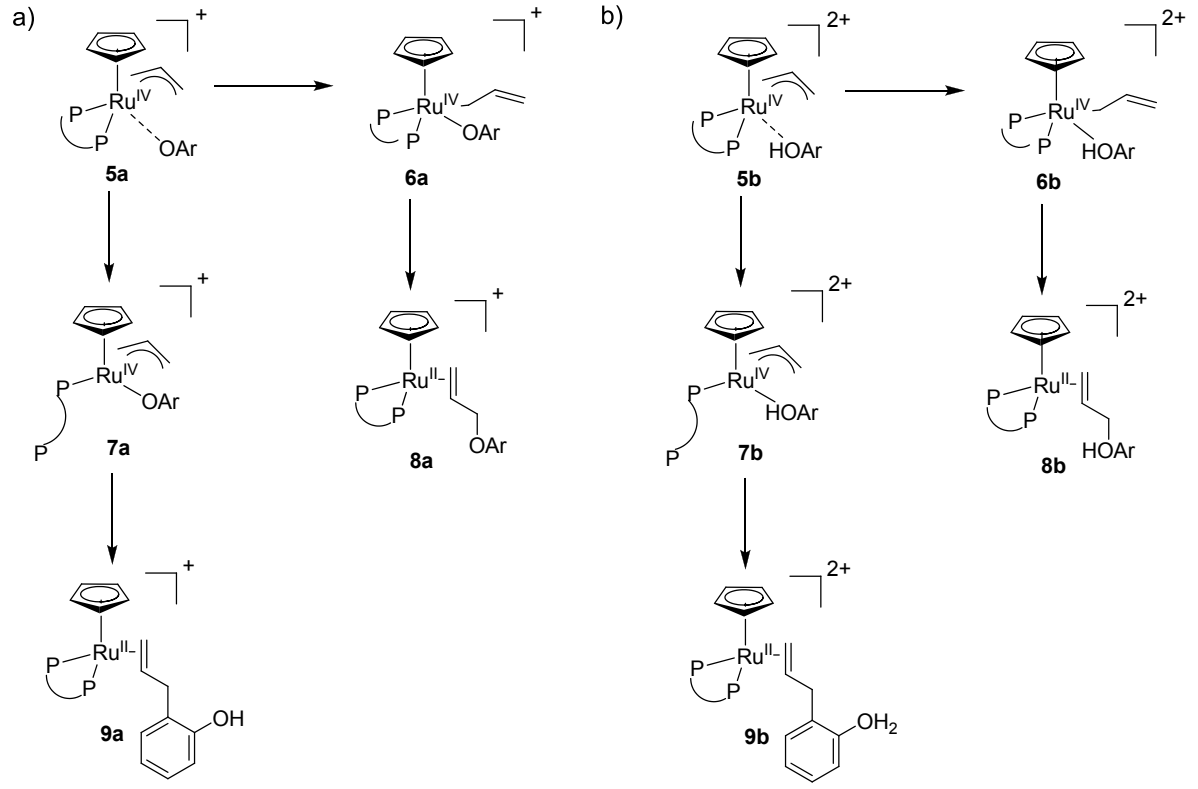


**Scheme 7.6.** Reductive elimination towards either O-allylated or C-allylated products.a) in absence of acid, b) in the presence of acid.

phenolate ion, especially in apolar solvents like toluene, coordination of the phenolate will compete with coordination of the phosphine and allyl ligand. Again, in order to prevent a highly unfavored 20-electron species, either the σ-allyl species **6a**-**6b** will be formed or phosphine dissociation will occur (**7a**-**7b**), depending on the stability of the chelate ring. From the σ-allyl species, reductive elimination can occur, which is the microscopic reverse of the oxidative addition of allyl ethers, forming ruthenium-bound allyl phenyl ether **8a**-**8b**. This reaction is highly exothermic, as expected for a microscopic reverse of a highly endothermic oxidative addition.

When instead of forming a σ-allyl species phosphine dissociation occurs (**7a**-**7b**), C-allylated products may be formed (**9a**-**9b**), as was discussed in Chapter 2 and 3. The molecular structures of the complexes resemble those obtained for the intermediates in oxidative addition (Figure 7.1) and are not discussed in detail. Similar to the oxidative addition step, both the monocationic complexes (Scheme 7.7a; absence of acid) as well as the dicationic complexes (Scheme 7.7b; presence of acid) were calculated.

### *7.2.6 Energy diagrams for reductive elimination*

**The cationic [RuCp(PP)(allyl)(OPh)]$^+$ system**

For the [RuCp(dpm)(allyl)(OPh)]$^+$ complex, in the absence of an acidic proton, the Ru(IV) intermediate in which one phosphine donor is dissociated (**7a**; Scheme 7.7a) lies considerably lower in energy than the Ru(IV)(σ-allyl) intermediate (**6a**), caused by the release of ring strain of the coordinated ligand as observed for the oxidative addition step (Scheme 7.4). Reductive elimination leads to either species **8a** or **9a**, of which the latter is thermodynamically favored. Since formation of **7a** is clearly favored, formation of **9a** is also more likely, which corresponds with the observation that [RuCp(dppm)]$^+$ selectively forms C-allylated product.

[RuCp(dpe)]$^+$ shows again an energy profile that is very different from that of [RuCp(dpm]$^+$. Intermediates **5a**, **6a** and **7a** have a relatively small energy difference and **7a** lies slightly higher in energy. This lack of preference corresponds with the experimental results reported in Chapter 2. The use of [RuCp(dppe)]$^+$ as a catalyst in the allylation of phenol shows no initial preference for either O- or C-allylation. The reductive elimination step is highly exothermic towards species **8a** and **9a** of which **9a** again is the lowest in energy (−35.0 and −46.9 kcal/mol respectively).

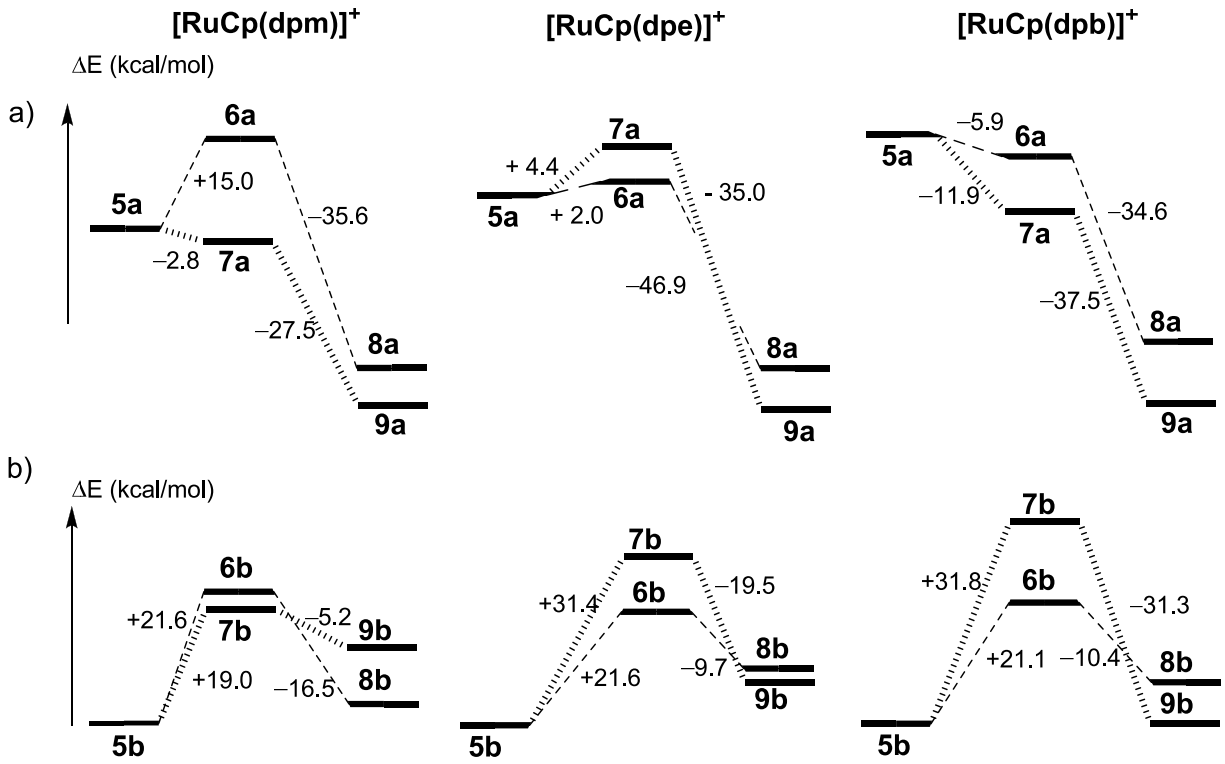


**Scheme 7.7.** Energy diagrams for the reductive elimination step towards [RuCp(PP)(allyl ether)]$^{n+}$ (**8**) and [RuCp(PP)(*o*-allylphenol)]$^{n+}$ (**9**) complexes in a) the absence of acid and b) the presence of acid.

Finally, the [RuCp(dpb)]$^+$ cationic species shows a lowering in energy going from **5a** to either **6a** or **7a**, of which the latter is lowest in energy in the absence of acid. Reductive elimination to form **8a** or **9a** is again highly exothermic (−34.6 and −37.5 kcal/mol respectively).

### The dicationic [RuCp(PP)(allyl)(HOPh)]$^{2+}$ system

In the presence of acid (Scheme 7.7b), isomerization of the very stable resting state **5b** to either **6b** or **7b** is a highly endothermic process for the three complexes (around + 20 to + 32 kcal/mol). This phenomenon indicates that from **5b** it is not likely that a phenol will coordinate onto the Ru(IV) center. The approach of a phenol molecule towards the Ru(IV) center must be accompanied by a simultaneous deprotonation and subsequent formation and coordination of a phenolate anion. It is interesting to see that the energy difference between **6b** and **7b** increases with increasingly larger bite angles. When the phenol approaches the Ru(IV) center, the increase in congestion of the ligands at Ru(IV) apparently favors π- to σ-allyl isomerization over phosphine dissociation. As it is proposed that O-allylation proceeds via a Ru(IV) σ-allyl species, this energy trend corresponds with the experimental observation that in the presence of acid complexes with large bite angles favor O-allylation over C-allylation. Reductive elimination from **6b** or **7b** leads to product-bound species **8b** and **9b** and is exothermic in all cases shown in Scheme 7.7 (−5 to −31 kcal/mol).

In the absence of acid product **8a** is always about 10 kcal/mol higher in energy than **9a**, as it should be according to the results shown in Scheme 7.2. In **8b** and **9b**, however, repulsion between the proton located at the O-atom of the substrate and the positively charged Ru(II) ion leads to the different energies of both **8b** and **9b** compared to the acid-free situation. In practice, with a catalytic quantity of protons, deprotonation will of course readily occur during the product forming step, preparing the proton for its action in the next catalytic cycle.

### *7.2.7 Total energy profile from substrates to products and discussion*

In Scheme 7.8, the oxidative addition and reductive elimination step for the $[RuCp(dpe)]^+$ complex are combined to illustrate the total energy profile of a catalytic phenol allylation pathway with allyl alcohol as the allylation agent. The pathway to O- and C-allylated product is given for both the monocationic (situtation a) as well as for the dicationic (situation b) catalyst system.

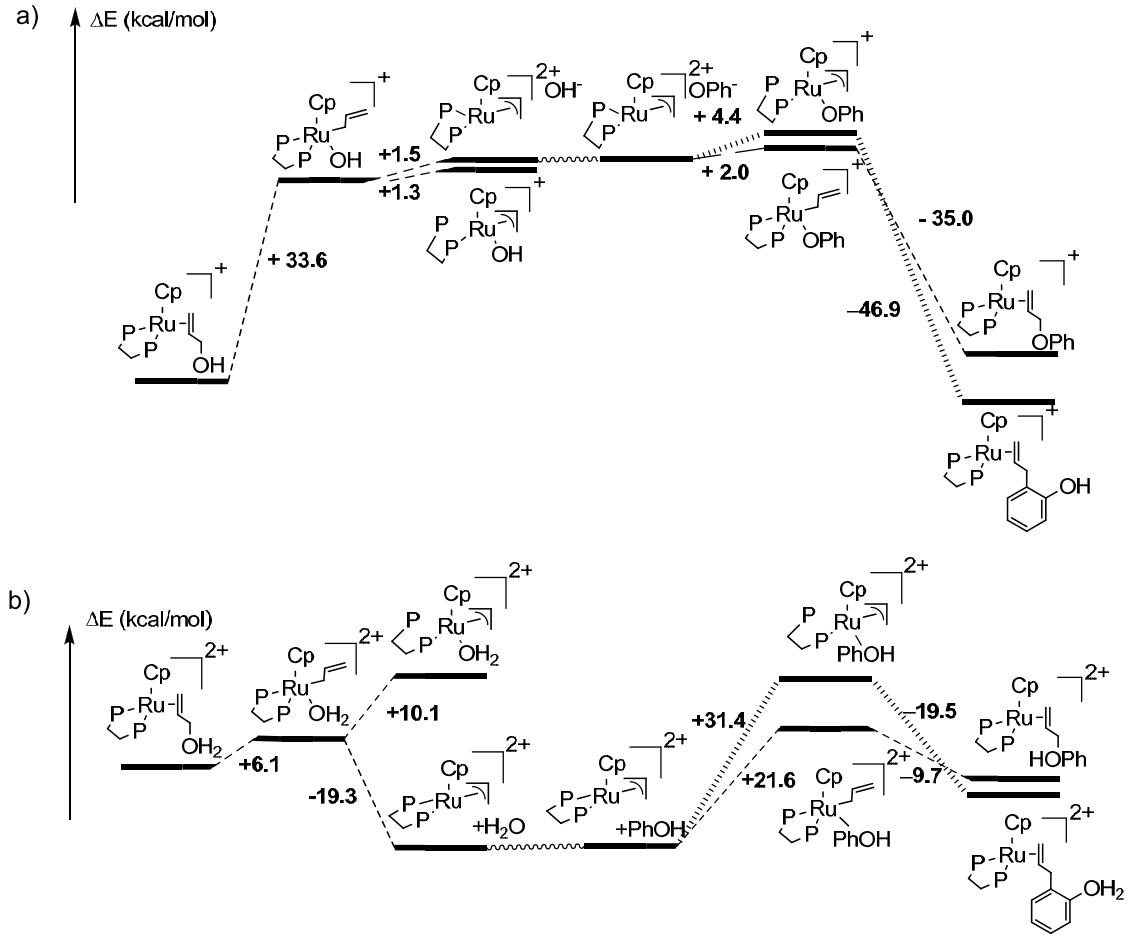


**Scheme 7.8.** Total energy profile of O- and C-allylation of phenol with allyl alcohol with $[RuCp(dpe)]^+$ as the catalyst a) in the absence and b) in the presence of acid.

For the cationic $[CpRu(dpe)(allyl\ alcohol)]^+$ system, the energy diagram is shown in Scheme 7.8a, simulating the catalyst system in the absence of acid. The endothermic oxidative addition towards Ru(IV), followed by the exothermic reductive elimination back to Ru(II) species is clearly observed. Although the energy difference due to exchange of the hydroxide anion with a phenolate anion is not taken into account, it is expected that this difference will be relatively small. The overall energy difference between initial and final state of the elementary reactions (+2.0 kcal/mol for O-allylation; −7.4 kcal/mol for C-allylation) must correspond with that of the overall reaction, shown in Scheme 7.2 (+ 0.1 kcal/mol for O-allylation; −8.8 kcal/mol for C-allylation).

For the dicationic $[RuCp(dpe)(allyl\ alcohol + H)]^{2+}$ system, simulating the presence of acid (Scheme 7.8b), such a correspondence with the overall allylation process, is less clear (−1.3 kcal/mol for both O- and C-allylation). Apparently, protonation of the coordinated allyl alcohol, but also the allyl phenyl ether and *ortho*-allylphenol changes the calculated energy differences between such species significantly. As indicated above, this can be seen as a limitation of the calculations as only fully protonated species have been calculated in Scheme 7.8b, while the protonation event itself cannot be calculated.

Nevertheless, even within the limitations set by DFT energy considerations several features of the phenol allylation reaction are satisfyingly illustrated. The promoting effect of protons on the oxidative addition by lowering its energy barrier is clearly observed, while the high stability of the $[Ru(IV)Cp(PP)(\pi\text{-allyl})]^{2+}$ species is also clearly recognized in the energy calculations. Furthermore, the competition between the various elementary organometallic process steps such as anion dissociation, dissociation of a phosphine moiety and $\sigma$-allyl$\rightarrow$ $\pi$-allyl rearrangement at the Ru centre are clearly rationalized as important activity- and selectivity-determining catalytic indicators.

The activation of allyl phenyl ether under product-forming conditions gives intermediates that again are involved in the same competitive elementary processes of anion- or phosphine dissociation and $\pi$-allyl $\rightarrow$ $\sigma$-allyl isomerization, ultimately leading to the thermodynamic C-allylated final product, unless the catalyst characteristics are such that the pathway towards C-allylated product is fully blocked. The present computational results are a rationalization of the notion that the pathway to C-allylated products requires ample coordination space at Ru(IV) made possible either by using small bite angle diphosphine ligands or ligands that form relatively labile chelates. It is suggested that ample accessible coordination space allows an initially O-coordinated phenoxy ligand to become strongly electrophilically activated by

Ru(IV) and thus to become attacked by the (bidentate) π-allyl moiety in the same coordination sphere forming C-allylated product (Chapters 2, 3). The alternative pathway of phenolate coordination to enforce π-allyl rearrangement into σ-allyl, and subsequent reductive elimination to allyl phenyl ether, cannot compete when ample space is available.

Apart from chelate stability of the bidentate ligands also their bulkiness will probably be important ligand parameters to limit accessible coordination space at the $[Ru(IV)Cp(PP)(allyl)]^{2+}$ center, such that phenoxyl coordination readily enforces a π-allyl to σ-allyl rearrangement. Steric and electronic properties of the ligand will be interrelated and their effects on catalytic performance may be difficult to predict; the DFT calculations presented in this chapter until now only involve $H_2P(CH_2)_nPH_2$ ligands, but it is clear that more advanced DFT calculations should be undertaken to investigate the predicted catalytic consequences of using "real life" ligands. Unfortunately, such extended ligand systems and their complexes were not within our computational possibilities.

One minor modification, relatively easy to handle computationally, involved the addition of methyl-substituents in the ligand backbone. In the next section the computational study of the effect of geminal substitution on the reductive elimination step is discussed.

### *7.2.8 Complexes having ligands with gem dialkyl substituted backbones*

In Chapter 3 it is reported that the incorporation of dialkyl geminal substituents in the diphosphine ligand backbone has a dramatic effect on especially the selectivity of the phenol allylation reaction.

It was proposed that geminal backbone substituents increase the chelate coordination stability and it was concluded that $[RuCp(PP)]^+$ complexes with stable chelating diphosphine ligands are more selective towards O-allylation. Especially the geminal dialkyl substitution of the ligand $C_1$- and $C_3$-backbones resulted in a dramatic increase in the selectivity of the catalysts for O-allylation. It would be interesting to corroborate this selectivity-improving effect of dialkyl substituents in the ligand's backbone by means of DFT-calculations.

The computational results discussed in the previous sections imply that the selectivity for allylation of phenols is primarily determined by the allyl phenyl ether reductive elimination, i.e. the product-forming step. Therefore, the focus of the calculations is on this step with hope to shed some light on the origin of this intriguing and subtle ligand effect on the selectivity in the allylation of phenols.

The energy profile of the reductive elimination of *o*-allyl phenol (**9a**) or allyl phenyl ether (**8a**) from a $[Ru(IV)Cp(PP)(allyl)(OPh)]^+$ species towards Ru(II)-bound product species, has been calculated for a Ru complex with a $C_1$- and $C_3$-geminal dimethyl-substituted bidentate phosphine ligand and is compared with the energy profile obtained with the respective unsubstituted ligands (Scheme 7.9).

For the unsubstituted dpm ligand it was calculated that species **7a** is lower in energy relative to **6a** (**6a** to **7a** = –17.8 kcal/mol). For the complex with the substituted 2,2-dpp ligand, phosphine dissociation upon phenolate coordination apparently is considerably less favored, since the energy difference between **6a** and **7a** is only –5.4 kcal/mol. The increased phosphine coordination strength towards Ru(IV) by *gem* dimethyl substitution at de $C_1$-backbone of dpm can be rationalized by the higher basicity at the phosphines due to the two electron-donating methyl substituents. The increase in chelate stability should indeed result in a catalyst which has a higher selectivity for O-allylation. However, as can be seen in Scheme 7.9a, phosphine

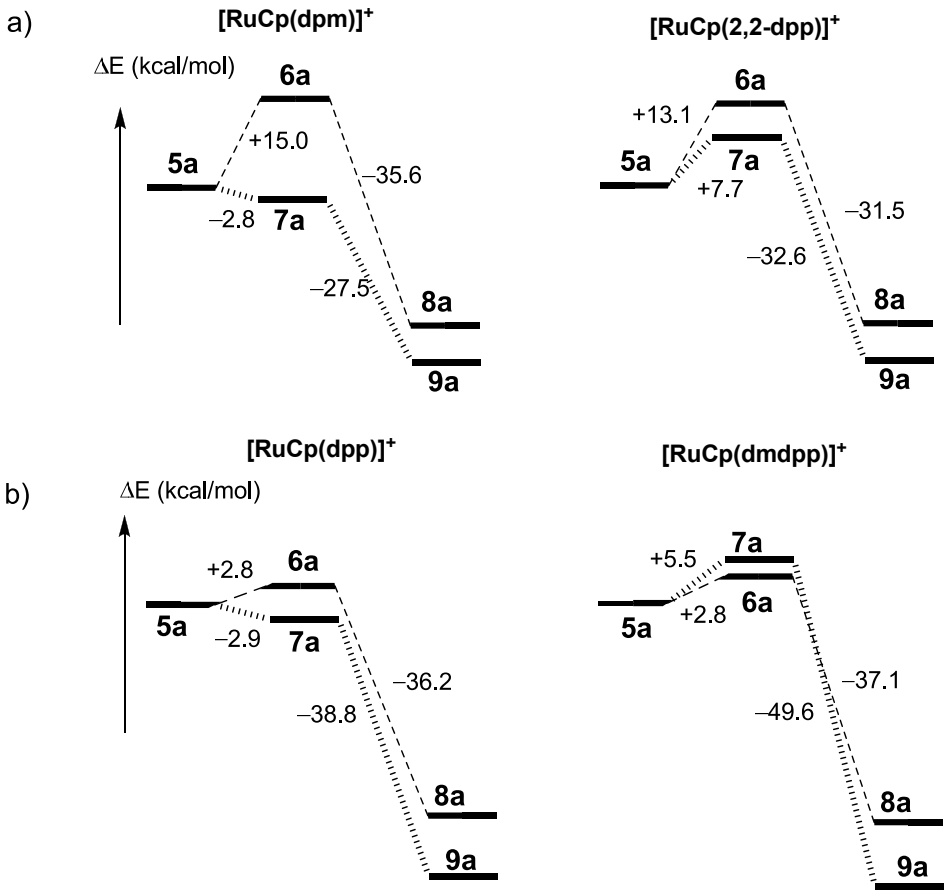


**Scheme 7.9.** Energy diagrams for the reductive elimination step for $[RuCp(PP)(allyl\ alcohol)]^+$ complexes in the absence of acid**.** Comparison between (a) $[RuCp(dpm)]^+$ (already shown in Scheme 7.3) and $[RuCp(2,2\text{-}dpp)]^+$, and (b) between $[RuCp(dpp)]^+$ and $[RuCp(dmdpp)]^+$.

dissociation upon phenolate coordination ultimately giving *o*-allylphenol (**9a**), still is about 5.4 kcal/mol advantaged over π-allyl → σ-allyl isomerization (**6a**). It thus appears that a consideration of the energy profiles alone, although directionally right, is quantitatively insufficient to explain the strong deviations in selectivity due to the *gem* substituents in the backbone of this catalyst's ligand.

It can be seen from Scheme 7.9b that diphosphine coordination of the $[RuCp(dmdpp)]^+$-complex is again somewhat stronger, i.e. dissociation of a phosphine moiety upon coordination of phenolate has a higher energy, compared to that of the $[RuCp(dpp)]^+$-complex. This could be due to an electronic effect at the phosphine donor or a slight structural difference of the energy-minimized configuration. Although in the catalytic pathway with the geminal substituted ligand phosphine dissociation upon phenolate coordination (pathway **5a** → **7a** → **9a** ) has only a slightly higher (< 3 kcal/mol) calculated energy barrier than the π-allyl → σ-allyl isomerization (pathway **5a** → **6a** → **8a** ), it is believed that the difference in energy profile is rather insignificant, although again directionally right, to explain the experimentally observed strong increase in O-allylation selectivity.

In addition to the DFT energy argument to compare the two reaction pathways, it is necessary to consider an entropic difference in the dissociation of one phosphine donor from Ru between the *gem* dimethyl-substituted and unsubstituted ligand complexes. Due to the restricted configurational freedom of the partial dissociated phosphine entity of the *gem*-dialkyl substituted ligand in **7a**, the entropy gain in dissociation of one phosphine donor must be significantly smaller than for the complex of the unsubstituted (flexible) ligand. Thus pathway **5a** → **7a** → **9a** becomes more unlikely to follow due to this unfavorable entropic factor in the *gem* disubstituted ligand. The importance of the entropy factor was already mentioned for the allylation vs isomerization effect with the $[RuCp(dpb)]^+$ complex. However, entropic effects are not taken into account with the standard DFT methodology applied here and more advanced DFT computational methods should be used to study the role of entropy also in the other elementary steps of the catalytic cycle.

## 7.3 Conclusions

With the theoretical data presented and supported with a vast quantity of experimental results described in the previous chapters, a detailed mechanistic picture is drawn that explains the observed features of the allylation of phenol with allyl alcohol using $[RuCp(PP)]^+$ complexes. Phosphine dissociation plays a crucial role in determining the activity and especially

selectivity of the catalysts and has a dramatic effect on the (de)stabilization of the energy levels of the intermediates in the catalytic cycle. The effects of changing the chelating phosphine ligand are observed for both the oxidative addition step as well as the reductive elimination, especially for the system calculated in the absence of acid. The system calculated in the presence of acid shows promotion of the oxidative addition step. The incorporation of *gem*-dialkyl substituted phosphine ligands in the catalysts stabilizes phosphine coordination in the Ru(IV) state, since phosphine dissociation becomes less favored. However, entropic effects will change the energy levels considerably, but these effects cannot be illustrated with the calculation method used here. Attempts should be undertaken to calculate these entropic effects with more detailed and extensive calculation methods.

## 7.4 Experimental

**Theoretical methods.** The potential energy surfaces (PESs) corresponding to the processes involved in the allylation of phenols with allyl alcohol have been explored using density functional theory (DFT)[12,13] with the Becke and Perdew (BP) functional.[14,15] All the geometry optimizations were carried out using Pople's 6-31G* (d,p) for H, C, O and P atoms[16] and the LANL2DZ effective core potential for ruthenium.[17-19] All of the geometrical parameters were fully optimized, and all of the structures located on the PESs were characterized as minima. No constraints to bonds, angles or dihedral angles were applied in the calculations, and all atoms were free to optimize. The SPARTAN '04 package (Wavefunction, Inc; www.wavefun.com) was used to carry out the calculations.

## 7.5 References


(1) Saburi, H.; Tanaka, S.; Kitamura, M. *Angew. Chem.-Int. Edit.* **2005**, *44*, 1730-1732.
(2) Nieves, I. F.; Schott, D.; Gruber, S.; Pregosin, P. S. *Helv. Chim. Acta* **2007**, *90*, 271-276.
(3) Onodera, G.; Imajima, H.; Yamanashi, M.; Nishibayashi, Y.; Hidai, M.; Uemura, S. *Organometallics* **2004**, *23*, 5841-5848.
(4) Bandini, M.; Eichholzer, A.; Kotrusz, P.; Tragni, M.; Troisi, S.; Umani-Ronchi, A. *Adv. Synth. Catal.* **2009**, *351*, 319-324.
(5) Nagashima, H.; Mukai, K.; Shiota, Y.; Yamaguchi, K.; Ara, K.; Fukahori, T.; Suzuki, H.; Akita, M.; Morooka, Y.; Itoh, K. *Organometallics* **1990**, *9*, 799-807.
(6) Gruber, S.; Zaitsev, A. B.; Worle, M.; Pregosin, P. S.; Veiros, L. F. *Organometallics* **2008**, *27*, 3796-3805.
(7) Piechaczyk, O.; Thoumazet, C.; Jean, Y.; le Floch, P. *J. Am. Chem. Soc.* **2006**, *128*, 14306-14317.
(8) Mora, G.; Piechaczyk, O.; Houdard, R.; Mezailles, N.; Le Goff, X. F.; le Floch, P. *Chem.-Eur. J.* **2008**, *14*, 10047-10057.
(9) O' Connor, J. M.; Casey, C. P. *Chem. Rev.* **1987**, *87*, 307-318.
(10) van Zeist, W. J.; Visser, R.; Bickelhaupt, F. M. *Chem.-Eur. J.* **2009**, *15*, 6112-6115.
(11) van der Drift, R. C.; Vailati, M.; Bouwman, E.; Drent, E. *J. Mol. Catal. A: Chem.* **2000**, *159*, 163-177.
(12) Koch, W.; Holthausen, M. C. *A Chemist's Guide to Density Functional Theory*; 2nd ed ed.; Wiley-VCH: Weinheim, 2000.

(13) Eichkorn, K.; Treutler, O.; Ohm, H.; Haser, M.; Ahlrichs, R. *Chem. Phys. Lett.* **1995**, *240*, 283-289.
(14) Becke, A. D. *Phys. Rev. A* **1988**, *38*, 3098-3100.
(15) Perdew, J. P. *Phys. Rev. B* **1986**, *33*, 8822-8824.
(16) Hehre, W. J.; Radom, L.; Schleyer, P. v. R.; Pople, J. A. *Ab initio Molecular Orbital Theory*; Wiley: New York, 1986.
(17) Hay, P. J.; Wadt, W. R. *J. Chem. Phys.* **1985**, *82*, 270-283.
(18) Wadt, W. R.; Hay, P. J. *J. Chem. Phys.* **1985**, *82*, 284-298.
(19) Hay, P. J.; Wadt, W. R. *J. Chem. Phys.* **1985**, *82*, 299-310.